Supporting information for

Rational design of a triiodide-intercalated dielectric-switching hybrid for visible-light absorption

Weichuan Zhang, Bo Kou, Peng Yu, Zhenyue Wu, Yunpeng Yao, Dhananjay Dey, Lina Li, and Junhua Luo *

Contents

1. Experimental

Sample preparation

Bismuth oxide (99.99 %) in a powder form Aladdin; Hydroiodic acid (55.0-58.0 %) and *n*-propylamine (99.99 %) in a liquid form were purchased from Aladdin.

1.25 grams of *n*-propylammonium and 1.55 grams of bismuth oxide were added to 15 mL of hydroiodic acid. The solution was completely dissolved after heating. After tens of minutes of slow cooling, the reddish-orange bulk single crystal (*n*-propylammonium)$_3$BiI$_6$ (**PB**) was obtained [CCDC 1847160 contains the supplementary crystallographic data for this paper. The data can be obtained free of charge from The Cambridge Crystallographic Data Centre via www.ccdc.cam.ac.uk/data_request/cif.]. To obtain the triiodide-intercalated dielectric hybrid of (*n*-propylammonium)$_4$·I$_3$·BiI$_6$ (**PTB**), the prototype solution was re-dissolved and recrystallized under an AM 1.5 simulated solar light at 6.3 mW cm^{-2}. Then black bulk crystals were obtained after ten hours.

Crystal structure determination

A transparent crystal of **PTB** was coated with oil, mounted on a loop, and transferred to a SuperNova four-circle diffractometer with a CCD plate detector for low temperature phase. Differently, the high temperature phase was collected using a Bruker D8 Venture diffractometer equipped with a Bruker APEX-II CCD detector. Unit-cell parameters were refined against all data. The crystal did not show significant decay during data collection. Frames were integrated and corrected for Lorentz and polarization effects using SAINT 8.27b and were corrected for absorption effects using SADABS V2012. [1] The space-group assignment was based on systematic absences, statistics, agreement factors for equivalent reflections, and successful refinement of the structure. The structure was solved by direct methods, expanded through successive difference Fourier maps using the Olex 2, and refined against all data using the SHELXTL software package.[2-5] Weighted R factors, R_w, and all goodness-of-fit indicators are based on F2. Thermal parameters for all atoms were refined anisotropically.

Powder X-ray diffraction

Powder X-ray diffraction (PXRD) for **PTB** was performed on a Miniflex600 X-ray diffractometer at different temperatures. The diffraction patterns were collected in the 2θ range of 5°−50° with a step size of 1°. The experimental power and film PXRD patterns obtained at room temperature, and simulated powder XRD pattern were acquired by the software of mercury.

UV-vis-NIR Diffuse Reflectance Spectroscopy

The UV-vis-NIR diffuse reflection data were obtained at room temperature and scan wavelength is between 200 nm and 1000 nm on a LAMBDA 950 UV/Vis Spectrophotometer. The BaSO4 powder sample was used as a standard (100% reflectance) and Absorption (K/S) data were calculated from the following Kubelka-Munk function: $K/S = (1–R)^2/2R$, where R is the reflectance, K is the absorption, and S is the scattering.[6]

Density Functional Theory Calculations

Density function theory (DFT) calculations were performed with the Cambridge Sequential Total Energy Package (CASTEP).[7, 8] The exchange-correlation functional was described by a generalized gradient approximation (GGA) with PerdewBurke-Ernzerhof functional for solids (PBEsol) scheme.[9] The interactions between the ionic cores and the electrons were described by the norm-conserving pseudopotential.[10] The following orbital electrons were treated as valence electrons: Bi 5d10 6s2 6p3; I 5s2 5p5; C 2s2 2p 2; N 2s2 2p3 and H 1s1. The numbers of plane waves included in the basis sets were determined by a cut-off energy 310 eV for **PTB**. To achieve the accurate density of the electronic states, the k-space integrations were done with Monk horst-Pack grids with a 3 × 4 × 6 k-point for **PTB**. The other parameters and convergent criteria were the default values of CASTEP code.

Differential scanning calorime measurements

The differential scanning calorime of **PTB** was performed using a NETZSCH DSC 200 F3 DSC instrument in the temperature range of 0-100 °C for seven cycle times. The crystalline samples were placed in aluminum crucibles that were heated and cooled with a rate of 10 K/min under the nitrogen atmosphere.

Thermogravimetric analyses

Thermogravimetric analyses were performed with a Netzsch TG 209 F1 Libra Thermo-Microbalance with alumina pans at a heating rate of 10 °C/min, using 10-mg samples.

Dielectric Constant Measurement

Dielectric constant tests were performed on the pressed-powder pellets that were covered by silver conducting glue. A Tonghui TH2828A analyzer was used to record the temperature variability of the real part (ε′) of **PTB** with frequencies of 50 and 100 kHz.

Conductivity Studies

Single crystal samples (~1.5 mm in length and ~0.5 mm in width) were cut to obtain smooth surfaces for conductivity Studies. Silver paint (PELCO was brushed onto both sides of the disk-shaped pellets to serve as the electrode. Current-Temperature curves of the device performed by a

Model 6517B Electrometer with a ST-102D Probe station. Electrical resistivity measurements were performed in air with a bias of 5 V in a temperature range of 325 K to 400 K.

The electrical conductivity (σ) can then be calculated as:

$$\rho = dI/VS$$

Where S is the uniform cross-section of the sample and d is the thickness of the sample.
The relationship between electrical conductivity, activation energy, and the temperature is shown in the following expressions:

$$\ln \sigma = \ln A - Ea/2kT$$

Where σ is the electrical conductivity, A is representative of Arrhenius type activation energy (negligible temperature dependence), Ea is the activation energy, k is the Boltzmann constant and T is the absolute temperature in Kelvin. From the equations, the activation energy can be determined by the slope of a logarithmic plot of σ versus 1/2kT.

Optoelectronic measurement

Current-voltage curves of the single-crystal device performed by a Model 6517B Electrometer with a ST-102D Probe station.

The density of trap for **PTB** single crystal was determined by using space charge limited current (SCLC) method. Planar single crystal devices were transected and sandwiched by two silver electrodes deposited on both sides to fabricate charge transport devices (Ag/**PTB**/Ag).

A typical logarithmic *I*–*V* trace of the stripped planar single crystal was measured by space charge limited current (SCLC) analysis.

Onset voltage for the TFL was used for determining the density trap:

$$n_{traps} = 2\varepsilon\varepsilon_0 V_{TFL}/ed^2$$

Where e is the electronic charge, d is the thickness of the crystal, ε= 13.2 is the relative dielectric constant of ***PTB*** which is determined by impedance analyzer, and ε_0 is the vacuum permittivity.

In addition, the hole mobility is well fitted by the Mott-Gurney law:

$$J_D = 9\varepsilon\varepsilon_0\mu V_b^2/8d^3$$

Where V_b is applied voltage.

Stability studies

Freshly prepared powder samples of **PTB** were placed on clean glass slides for this experiment. For the humidity study, a sample was placed in a plastic box in dark and the relative humidity was maintained at ~50% humidity.

Figures

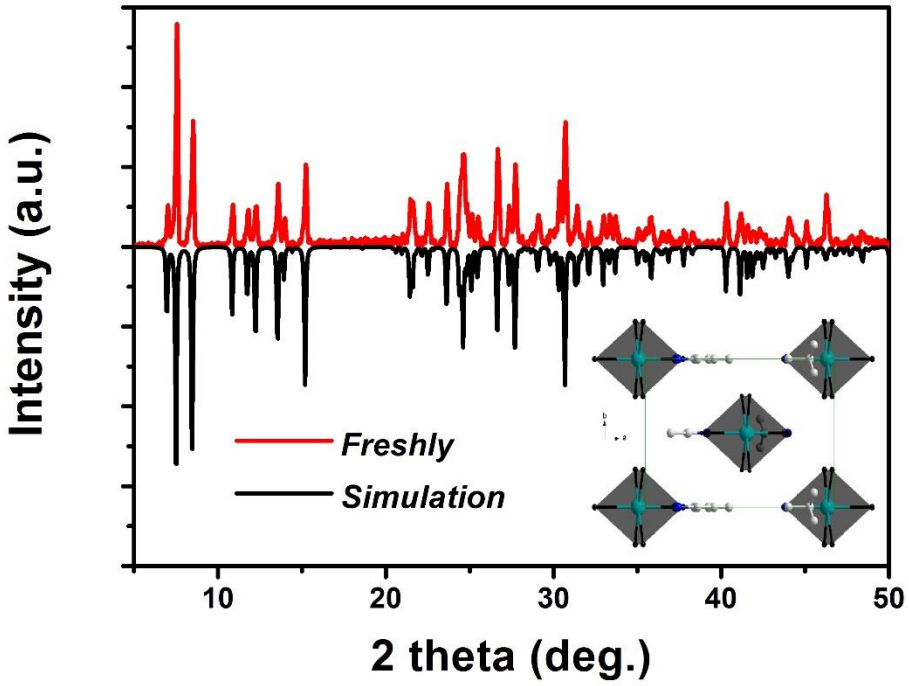

Fig. S1 X-ray diffraction patterns for **PB**.

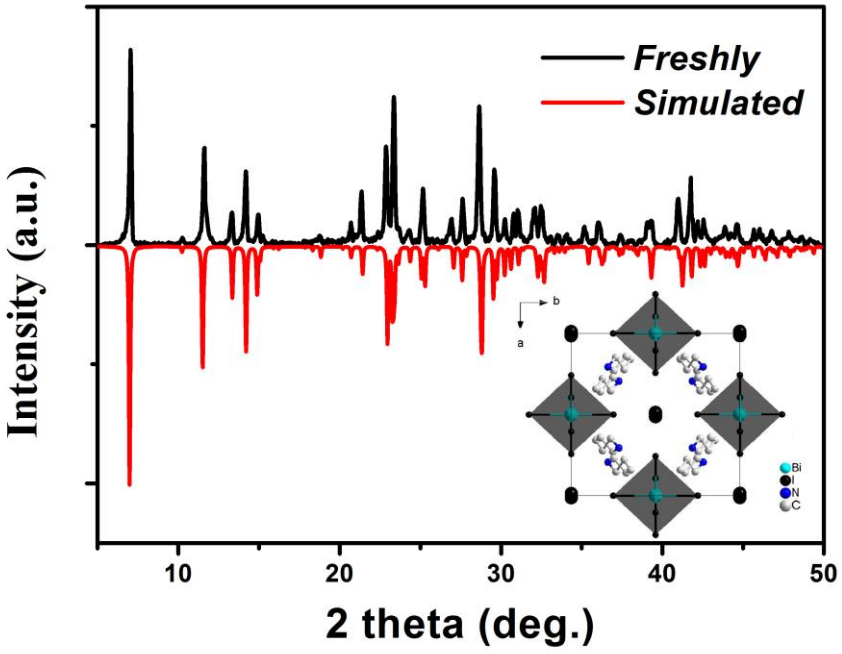

Fig. S2 X-ray diffraction patterns for **PTB**.

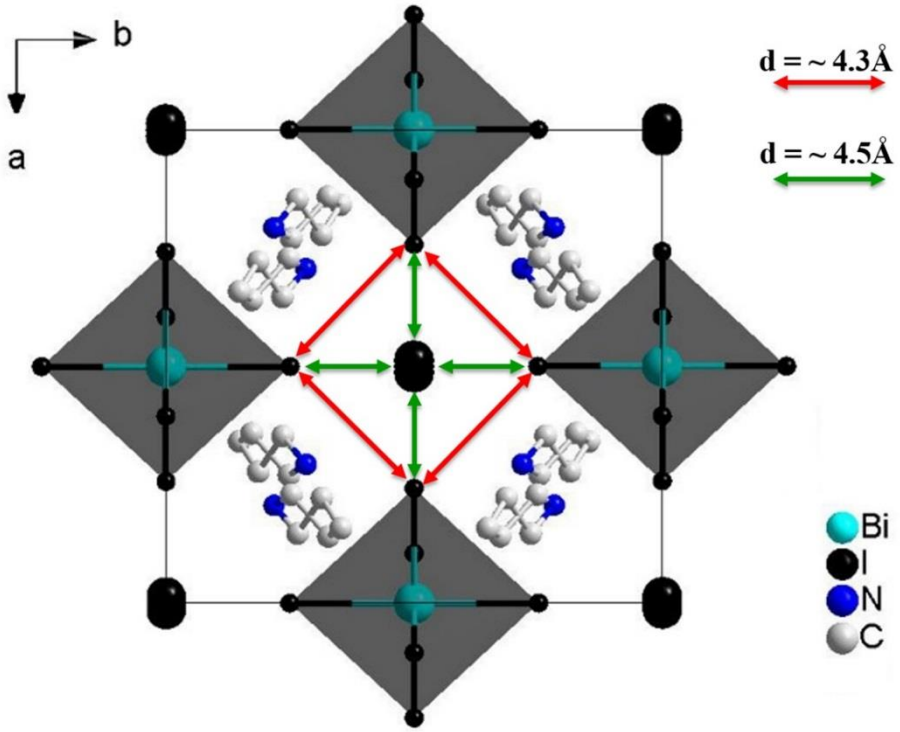

Fig. S3 The interanionic I···I distances between triiodides and metal halides (4.3 Å) are comparable to that the inorganic clusters of [BiI6]3- anionics (4.5 Å). Hydrogen atoms were omitted for clarity.

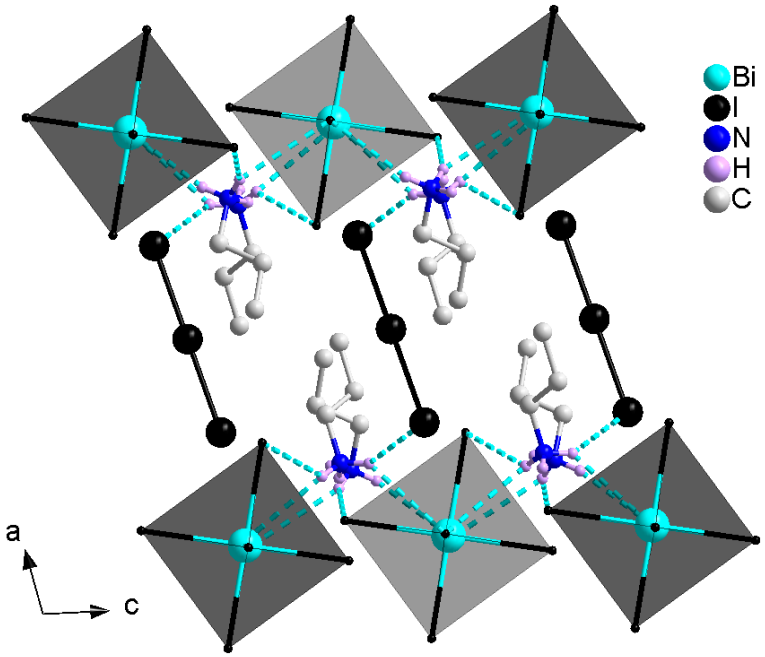

Fig. S4 N-H···I hydrogen bonds of the inorganic clusters and organic cations, as shown by blue dashed lines.

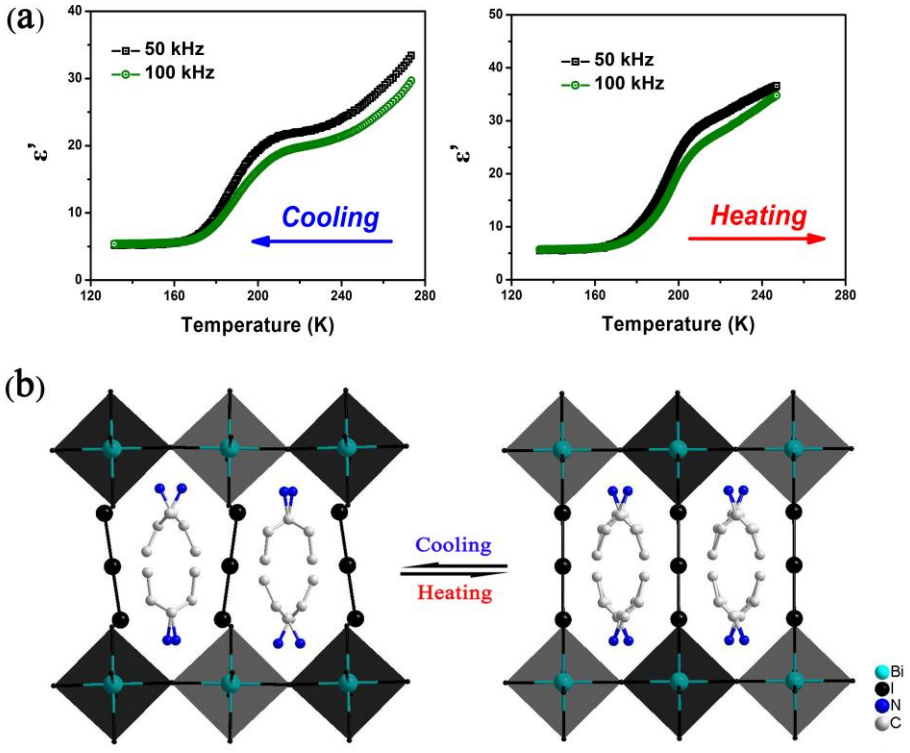

Fig. S5 (a) Temperature-dependent dielectric constants, determining by pressed-powder pellets. (b) Molecular structures at different temperatures: Perspective view along the c-axis at the low- and high-temperature phases. Hydrogen atoms were omitted for clarity

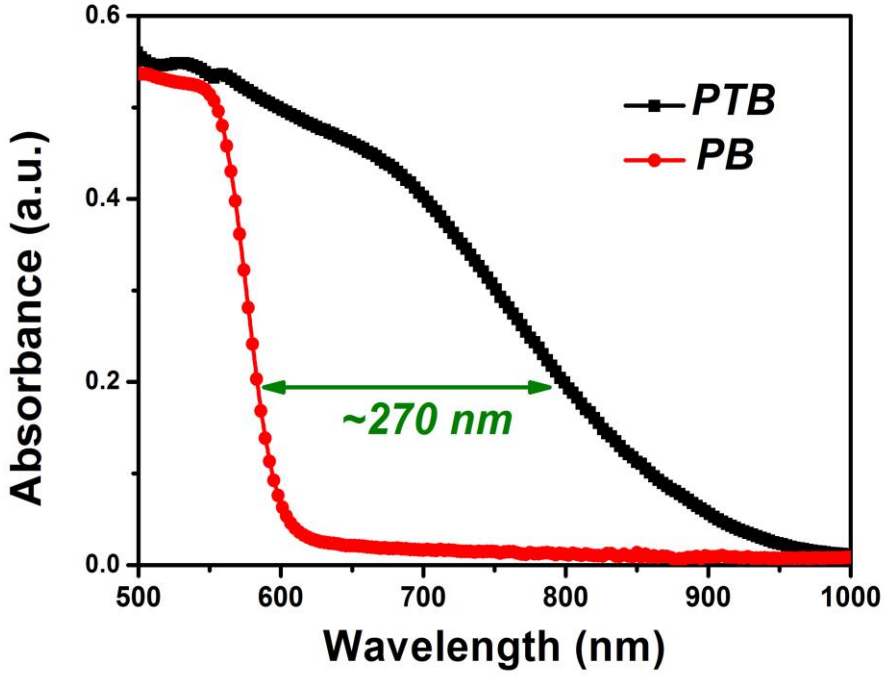

Fig. S6 Absorption spectra of single crystal samples.

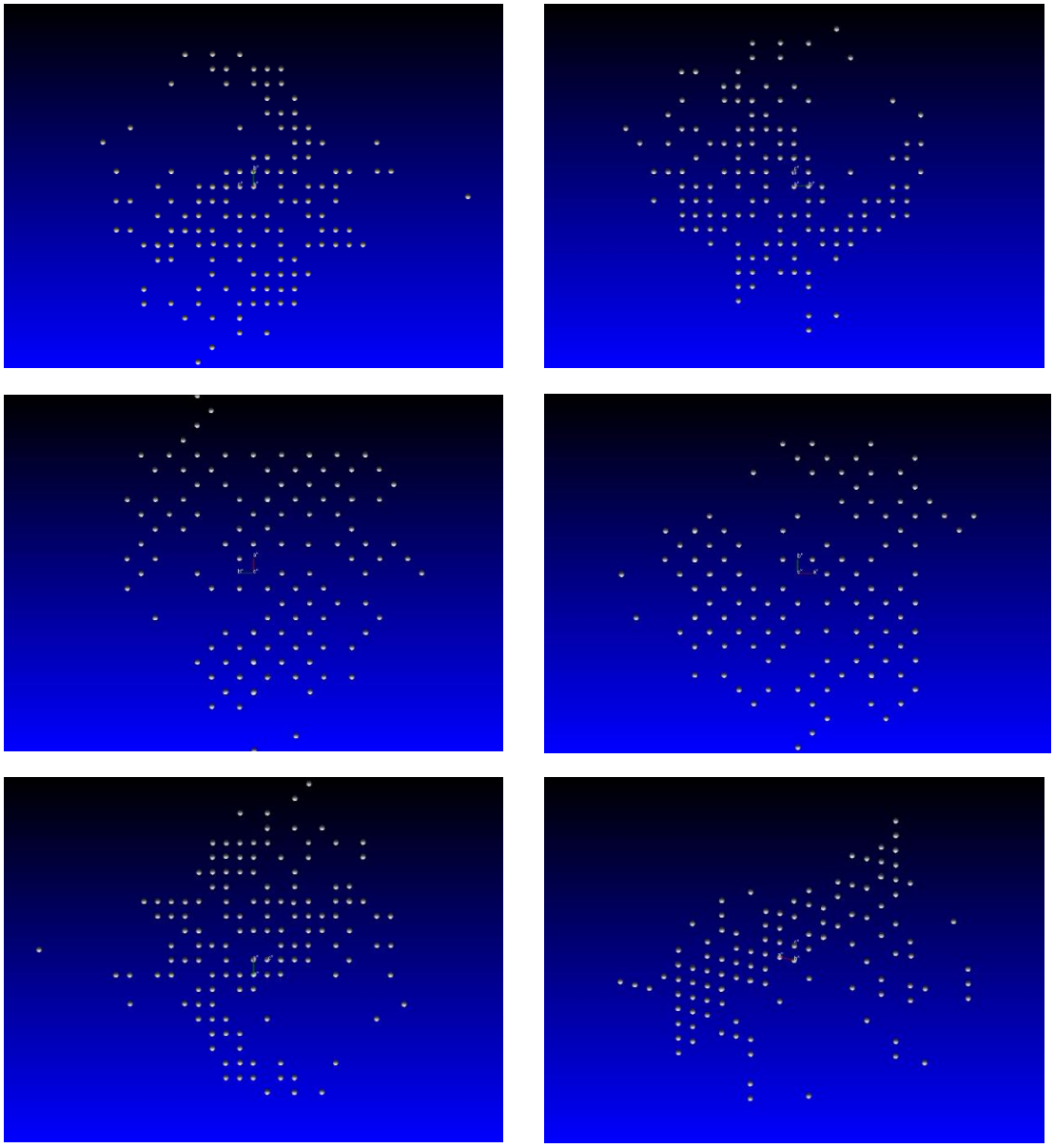

Fig. S7 The reciprocal space mapping of single crystal, which clearly indicates the excellent crystal quality without any defective pixel.

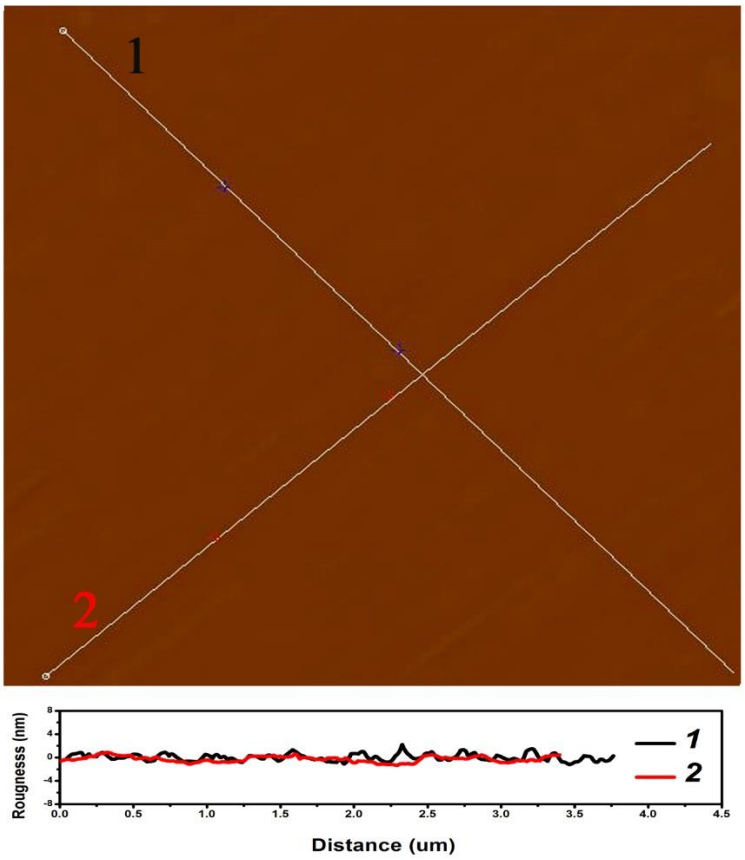

Fig. S8 AFM image of the single-crystal surface.

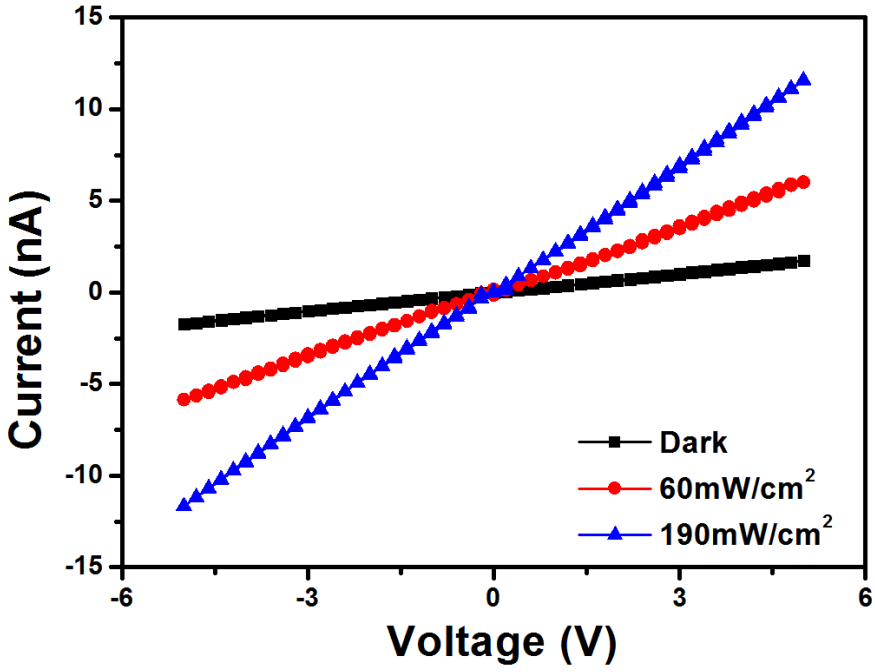

Fig. S9 Current–voltage curves of the **PTB** single crystal photodetector in dark and under illumination with a 405nm laser different light intensities.

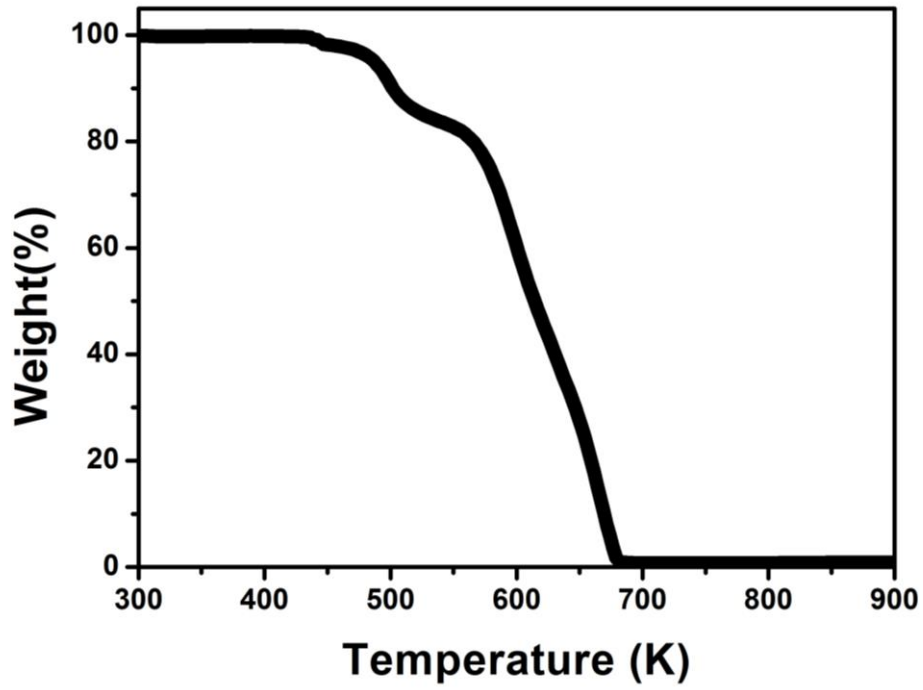

Fig. S10 Thermal stability of **PTB** measured by TGA method, showing a high thermal stability up to 429K.

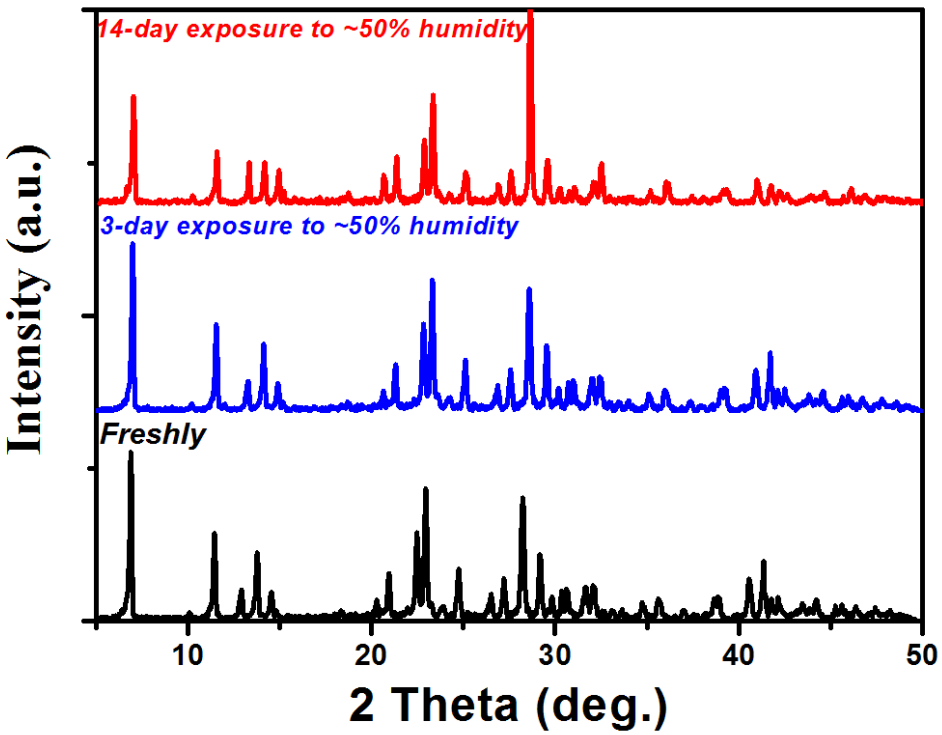

Fig. S11 PXRD patterns of **PTB** after exposure to humidity.

Tables

Table S1. Selected crystal data at 100 and 210 K.

Empirical formula	$(C_3H_{10}N)_4 \cdot I_3 \cdot BiI_6$	
Formula weight	1591.56	1591.56
Temperature/K	100 (4)	210
Crystal system	monoclinic	monoclinic
Space group	$P2_1/n$	C2/m
a/Å	12.5733(4)	12.0240(7)
b/Å	12.1377(3)	12.3072(8)
c/Å	11.9395(3)	12.6205(8)
α/°	90	90
β/°	102.720(3)	102.258(2)
γ/°	90	90
Volume/$Å^3$	1777.38(9)	1825.0(2)
Z	2	2
$\rho_{calc}g/cm^3$	2.974	2.896
μ/mm^{-1}	12.784	12.450
F(000)	1400.0	1400.0
Radiation (MoKα)	0.71073	0.71073
2Θ range for data collection/°	6.644 to 59.462	4.792 to 55.02
Reflections collected	20352	16367
Data/restraints/parameters	4492/0/125	2185/3/88
Goodness-of-fit on F^2	1.048	1.276
Final R indexes [I>=2σ (I)]	0.0236	R_1 = 0.0406
R_1[a] &wR_2[b]	0.0397	wR_2 = 0.1098
CCDC NO.	1847121	1847122

[a] $R(F_o) = \sum||F_o| - |F_c||/\sum|F_o|$. [b] $R_w(F_o) = (\sum_w||F_o| - |F_c||^2/\sum|F_o|^2)^{1/2}$, $w = [\sigma^2(F_o) + (0.002F_o)^2]^{-1}$

NOTE: The CIF file contains three **PTB** structure, which was collected at 100, 210 and 300K. CCDC numbers are 1847121, 1847122 and 1869781 respectively.

Table S2. Selected bond lengths (Å) and bond Angles (°) of the low temperature phase.

Bond lengths (Å)	Bond Angles (°)
Bi1 I3 3.0731(3)	I3 Bi1 I3 180.0 3_766
Bi1 I3 3.0731(3) 3_766	I3 Bi1 I4 90.253(6). 3_766
Bi1 I4 3.0742(3)	I3 Bi1 I4 89.747(6)
Bi1 I4 3.0741(3) 3_766	I3 Bi1 I4 90.253(6) 3_766
Bi1 I5 3.0582(3)	I3 Bi1 I4 89.748(6) 3_766 3_766
Bi1 I5 3.0581(3) 3_766	I4 Bi1 I4 180.0 3_766
I2 I6 2.9333(3)	I5 Bi1 I3 91.154(7) 3_766
I6 I2 2.9333(3) 3_667	I5 Bi1 I3 88.846(8) 3_766 3_766
	I5 Bi1 I3 91.155(8) 3_766
	I5 Bi1 I3 88.845(8)
	I5 Bi1 I4 90.064(7) 3_766
	I5 Bi1 I4 89.936(7)
	I5 Bi1 I4 89.936(7) 3_766 3_766
	I5 Bi1 I4 90.063(7) 3_766
	I5 Bi1 I5 180.0 3_766
	I2 I6 I2 180.0 3_667

Table S3. Selected bond lengths (Å) and bond Angles (°) of the high temperature phase.

Bond lengths (Å)	Bond Angles (°)
Bi1 I1 3.0770(6)	I1 Bi1 I1 180.0 5_766
Bi1 I1 3.0770(6) 5_766	I1 Bi1 I2 90.0 5_766
Bi1 I2 3.0847(6) 5_766	I1 Bi1 I2 90.0 5_766 5_766
Bi1 I2 3.0847(6)	I1 Bi1 I2 90.0 5_766
Bi1 I3 3.0744(7) 5_766	I1 Bi1 I2 90.0
Bi1 I3 3.0744(7)	I2 Bi1 I2 180.0 5_766
I4 I5 2.9374(12) 5_665	I3 Bi1 I1 91.471(19). 5_766
I4 I5 2.9375(12)	I3 Bi1 I1 88.529(19) 5_766 5_766
	I3 Bi1 I1 88.530(19)
	I3 Bi1 I1 91.471(19) 5_766
	I3 Bi1 I2 90.0 5_766 5_766
	I3 Bi1 I2 90.0 5_766
	I3 Bi1 I2 90.0 5_766
	I3 Bi1 I2 90.0
	I3 Bi1 I3 180.0 5_766
	I5 I4 I5 180.0 5_665

References

1 SAINT and SADABS (Bruker AXS Inc., Madison, Wisconsin, 2007).

2 G. M. Sheldrick, *Acta Cryst. Sect. A*, 2008, **64**, 112.

3 P. Muller, R. Herbst-Irmer, A. L. Spek, T. R. Schneider, M. R. Sawaya, Crystal structure refinement: A crystallographer's guide to Shelxl; Oxford University Press, 2006.

4 G. Sheldrick, *Acta Cryst. Sect. C* 2015, **71**, 3.

5 O. V. Dolomanov, L. J. Bourhis, R. J. Gildea, J. A. K. Howard, H. J. Puschmann, *Appl. Crystallogr.* 2009, **42**, 339.

6 P. Kubelka, F. Z. Munk, *Tech. Phys.* 1931, **12**, 593.

7 M. D. Segall, *J. Phys.: Condens. Matter*, 2002, **14**, 2717.

8 S. J. Clark, M. D. Segall, C. J. Pickard, P. J. Hasnip, M. J. Probert, K. Refson, M. C. Payne, *Z. Kristallogr. Cryst. Mater* 2005, **220**, 567.

9 J. P. Perdew, A. Ruzsinszky, G. I. Csonka, O. A. Vydrov, G. E. Scuseria, L. A. Constantin, X. Zhou, K. Burke, *Phys. Rev. Lett.* 2008, **100**, 136406.

10 D. R. Hamann, M. Schlüter, C. Chiang, *Phys. Rev. Lett.* 1979, **43**, 1494.